Fermilab FERMILAB-TM-2204 March 2003

The Tevatron Transverse Dampers

Cheng-Yang Tan
Jim Steimel

Beams Division/Tevatron

ABSTRACT: We describe in this paper the theory and construction of the Tevatron transverse dampers. The goal of these dampers is to keep the beam stable when we operate at lower chromaticities. The reason for operating at lower chromaticities is to improve the beam lifetime. However, the beam becomes unstable at low chromaticies and thus dampers are required. Also included in this paper are the damper commissioning notes and their real-life performance.

INTRODUCTION

The motivation for building transverse dampers for the Tevatron is to improve the lifetime of the proton and pbar beam on their helices during pbar injection. Previous studies by Y. Alexahin *et al* [1], showed that when octupoles were used to stabilize the beam, and chromaticities lowered, the lifetime of the beam of both species on the helix is improved. However, due to great difficulties in using octopoles in operations because of drifts in tunes, coupling and chromaticities at 150 GeV, this method was abandoned from use in operations. Therefore, when it was decided to resurrect the idea of lowering the chromaticity to improve beam lifetimes, we had to come up with some other way of keeping the beam stable and transversely damping the beam immediately came to mind.

The idea behind lowering the chromaticity ξ comes from the simple observation that the tune spread ΔQ is related to the energy spread dp/p by

$$\Delta Q = \xi dp/p \tag{1}$$

Thus, if the chromaticity is lowered, ΔQ is smaller and the beam will occupy a smaller footprint in the tune plane. A smaller footprint means that the beam will enclose fewer resonances which means that less beam will be lost and thus the lifetime is improved. However, there is a competing mechanism which throws a spanner into this. As long as there is a non-zero transverse impedance, the beam naturally becomes more unstable when the tune spread becomes smaller because Landau damping becomes weaker. Stability is determined by the Keil-Schnell stability criteria which is given by [2]

$$|(\Delta\omega_q)_{\rm coh}| \lesssim (\Delta\omega_q)_{\rm HWHM} F \tag{2}$$

where $(\Delta\omega_q)_{\rm coh}$ is the coherent betatron tune shift which comes from the transverse impedance, $(\Delta\omega_q)_{\rm HWHM}$ is the betatron tune spread measured at half-width half-max

and F is the form factor depending on distribution. $F = 1/\sqrt{3}$ for an elliptic distribution. This tells us that when we lower the chromaticity, which decreases $(\Delta\omega_q)_{\rm HWHM}$, at some point $|(\Delta\omega_q)_{\rm coh}|$ becomes larger than the rhs of (2), and the beam becomes unstable. Therefore, in order to keep the beam stable when we lower the chromaticity, we have to have a stabilization mechanism and in this case we choose to use active transverse damping.

In practice, for (36×36) bunch high energy physics operations after August of 2002, with both the horizontal and vertical dampers in service, the chromaticities of the horizontal plane is lowered by 6 units and the vertical plane by 4 units from their nominals which is about 8 for both planes on the central orbit and about 12 units for horizontal and 8 units for the vertical on the proton helix.

Table 1. Parameters of the Tevatron

Symbol	**Description**	**Value**
h	harmonic number	1113
–	# of bunches	36
–	# buckets between bunches in a train	21
–	# buckets between trains	140
f_r	revolution frequency at 150 GeV	47.712 kHz
$f_{\rm RF}$	frequency of RF drive at 150 GeV	53.103639 MHz
f_r	revolution frequency at 980 GeV	47.713 kHz
$f_{\rm RF}$	frequency of RF drive at 980 GeV	53.104705 MHz
q_h	fractional horizontal tune	0.583 f_r
q_v	fractional vertical tune	0.575 f_r

Since the setup for damping in either plane is identical (except for pickups and kickers), we will only discuss the horizontal dampers in this paper. And before we plough on with

the theory, setup and results, the relevant parameters of the Tevatron are shown in Table 1 and the Fourier transform pairs which we will use throughout this paper are

$$\left.\begin{aligned} \tilde{F}(\omega) &= \int_{-\infty}^{\infty} dt\; e^{-i\omega t} f(t) \\ f(t) &= \frac{1}{2\pi} \int_{-\infty}^{\infty} d\omega\; e^{i\omega t} \tilde{F}(\omega) \end{aligned}\right\} \tag{3}$$

The choice of these Fourier transform pairs are dictated by the Hewlett Packard vector signal analyzer which we use to measure the frequency responses of the damper system.

THEORY

Let us consider a simple damper system shown in Figure 1. The source of this derivation comes from McGinnis [3]. Looking at Figure 1, Z_E represents the impedance of the electronics and G_B represents the conductance of the beam. Therefore,

$$I_G = G_B V_{\text{out}} \tag{4}$$

and the output voltage V_{out} of the damper is

$$\left.\begin{aligned} V_{\text{out}} &= Z_E\Big(I_{\text{in}} + I_G\Big) \\ &= Z_E\Big(I_{\text{in}} + G_B V_{\text{out}}\Big) \end{aligned}\right\} \tag{5}$$

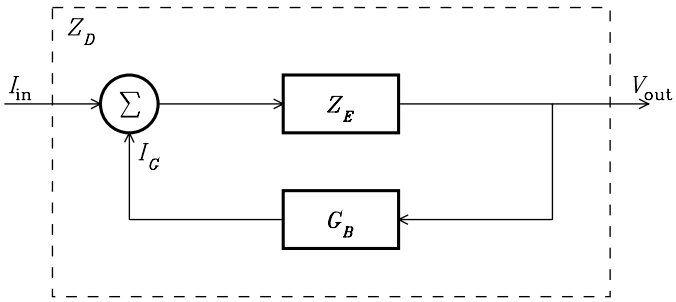

Figure 1 This is a block diagram of a simple damper system.

Solving for the impedance of the entire system Z_D, we have

$$Z_D(s) = \frac{V_{\text{out}}}{I_{\text{in}}} = \frac{Z_E(s)}{1 - G_B(s)Z_E(s)} \tag{6}$$

So, if we examine (6), we can see in its denominator is $G_B Z_E$, which is the open loop response of the damper system. To determine the stability of the damper system, let Z_E be of finite bandwidth with one pole, i.e.

$$Z_E \equiv \frac{Z'_E}{1 + \alpha s} \tag{7}$$

Then

$$Z_D = \frac{Z'_E}{\alpha\left(s + \frac{1-G_B Z'_E}{\alpha}\right)} \tag{8}$$

which implies that the pole is at

$$s_p = -\frac{1 - G_B Z'_E}{\alpha} \tag{9}$$

and thus by inverse Laplace transforming (8), we have the temporal response W_D of the damper system

$$\left.\begin{aligned} W_D(t) &\sim e^{s_p t} \\ &= e^{-\frac{1-\mathrm{Re}\left[G_B Z'_E\right]}{\alpha} t} \times e^{i\mathrm{Im}[G_B Z'_E]t} \\ &= (\text{decay or growth part}) \times (\text{oscillatory part}) \end{aligned}\right\} \tag{10}$$

Clearly, for dampers we want the decay part of (10), thus

$$1 - \mathrm{Re}\left[G_B Z'_E\right] > 0 \tag{11}$$

or

$$\mathrm{Re}\left[G_B Z'_E\right] < 1 \tag{12}$$

which means that the real part of the open loop response must be < 1 for damping. This is the most important result of this section.

SETUP

In this section, we will go through each part of our setup used for our bunch by bunch transverse dampers and show that the open loop response $G_B Z'_E < 1$. Figure 2 is a block diagram of the setup. The damper system starts at the stripline pickups working in difference mode. A transverse kicker is installed at a position in the Tevatron so that it has a phase advance of of an odd multiple of $\pi/2$ w.r.t. pickup. In order to improve the dynamic range of the damper system, a method developed by McGinnis called the autozero circuit shown in Figure 4, is used to virtually centre the beam in the pickup. This signal is mixed down with the Tevatron RF and low pass filtered to produce a transverse position error signal. The error signal is processed with electronics which perform the following:

(i) Suppress the revolution harmonics so that the damper does not fight the closed orbit.

(ii) Add delay $(T + t_{pk})$ where T is the revolution period and t_{pk} is the transit time from the pickup to the kicker, so that when the pickup detects the signal of bunch 1 it will kick bunch 1 one turn later.

Note that since the delay is $(T+t_{pk})$, the phase advance ϕ_{pk} between pickup to kicker is $-\Delta\omega_q(T+t_{pk})$ where ω_q is the tune frequency. The negative sign comes from the definition of the Fourier transform.

Every block circuit described above and in Figure 2 will be analyzed further in the following subsections.

Autozero Circuit

The autozero circuit was developed by McGinnis to improve the dynamic range of the damper system. If the closed orbit of the beam is not in the electrical centre of the

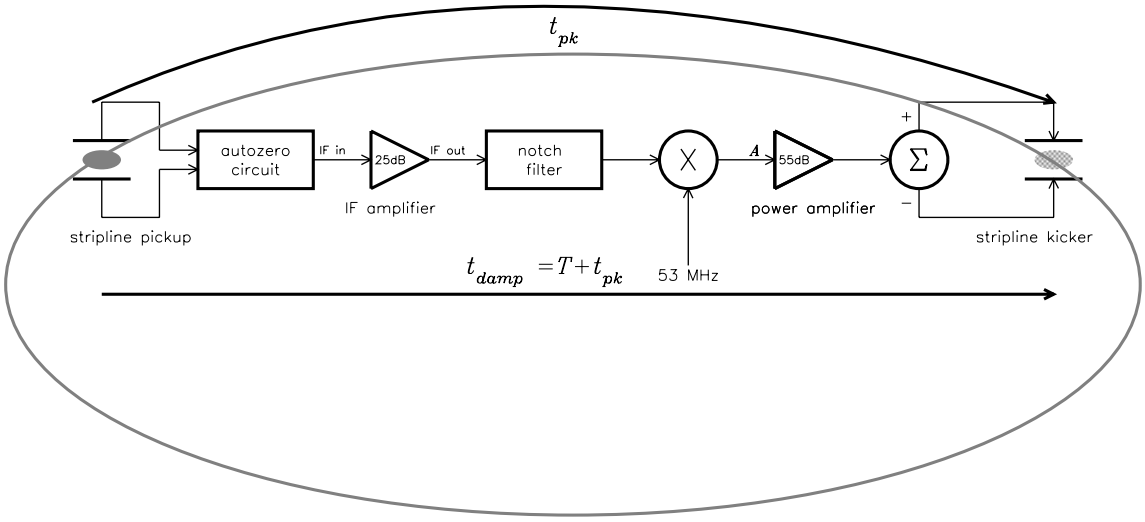

Figure 2 This is a block diagram which shows the overall setup of the transverse damper system. Note that the signal of the bunch which is detected at the stripline pickup is applied approximately one turn later to the same bunch at the stripline kicker. Each block is expanded further in Figures 4 and 5.

striplines, then clearly the induced voltage on plate A, V_A is not equal to the voltage V_B on plate B. See Figure 3. However, by changing the value of the attenuator connected on plate B, we can make $V_A = V_B$. Thus, the beam is now virtually centred in the stripline pickup and the dynamic range is immediately improved because we have essentially removed the DC component of the error signal, i.e. we can have much more gain downstream without saturating the amplifiers due to the DC component.

In order to change the attenuation on plate B without human intervention, a feedback loop is built to automatically turn the variable attenuator to minimize the DC component. This is called autozeroing. We refer to both Figures 3 and 4 in our description. The

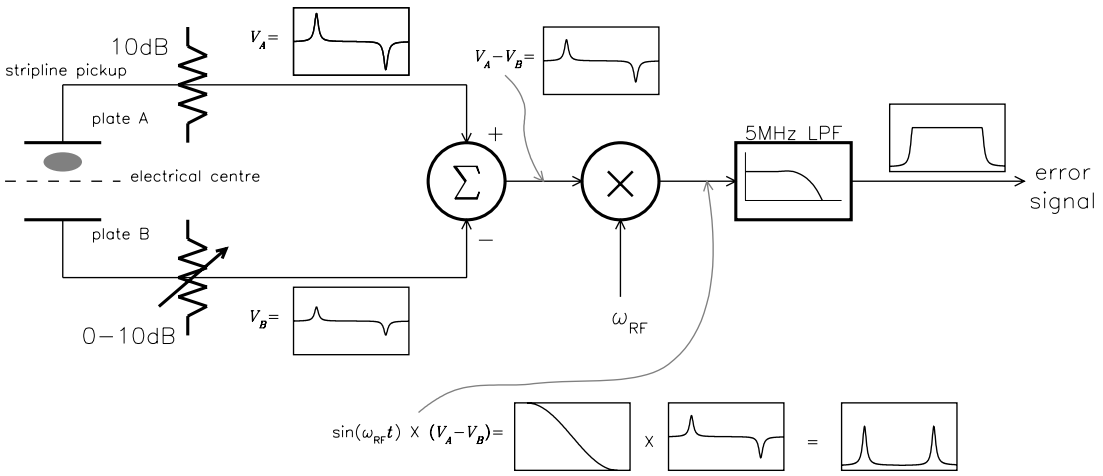

Figure 3 The mix down process which produces the autozero error signal is shown here. The massaged signal is drawn at the output of each device.

doublets on plates A and B are sent into the summer and then mixed down with the RF. The mixer when phased correctly, flips the sign of one half of the doublets so that they look like two peaks. These two peaks go through a low pass filter which smears out the region between the peaks so that it looks flat. This is where sample and holding can be applied. The sample and held signal is sent into another low pass filter which has a roll off frequency which is much lower than the tune frequency so that transverse motions of the beam which are slower than the betatron motion are corrected. The error signal is checked against a window threshold set by the user. If the error signal is outside the window threshold, the variable attenuator is rotated in the appropriate direction until the error signal is within the window boundaries. In this setup, the motor moves at full speed in either direction and so the feedback filter must not be too small.

Even with the motor moving at full speed, the autozero circuit is the slowest part in the damper circuit because it takes ~ 0.5 s for the attenuator to rotate from its position

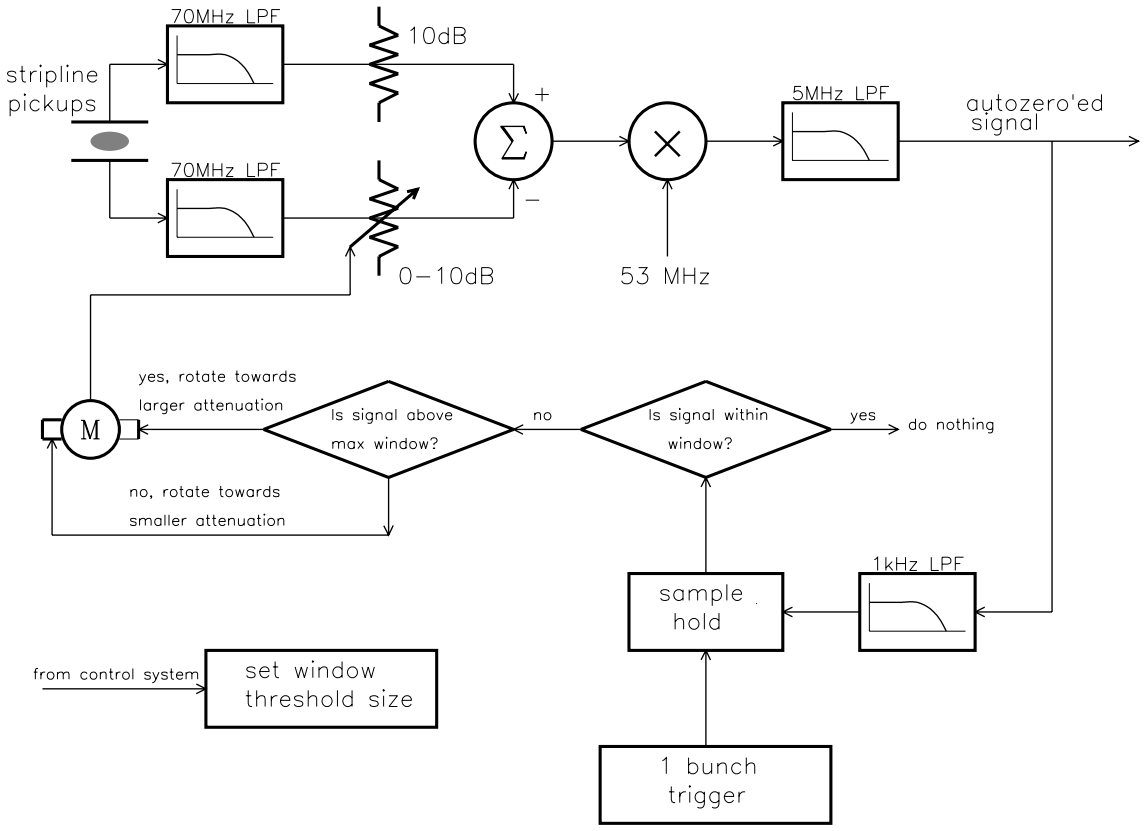

Figure 4 This figure shows the block diagram of the autozero circuit.

when the beam is on the central orbit to its position when the beam is on the helix which is ~ 8 mm w.r.t. the central orbit.

Digital Notch Filter

The digital notch filter consists of two digital delay lines when summed together produces notches at the revolution harmonics. Its response is given by

$$R_{\text{notch}}(\omega) = 1 - e^{-i\omega NT} \tag{13}$$

where T is the revolution period and N is the number of revolution periods in the delay.

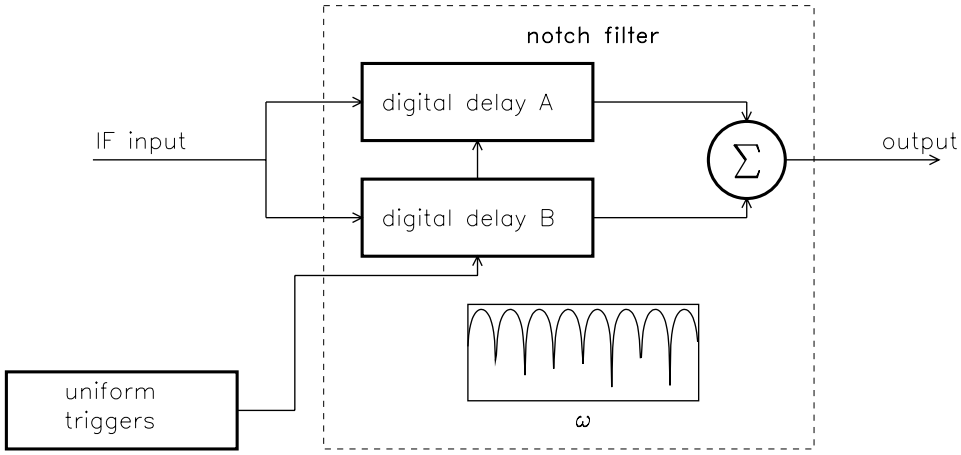

Figure 5 The digital notch filter.

The notch filter clearly suppresses the revolution harmonics at $\omega_r = 2\pi f_r$ since $R_{\text{notch}} = 0$ whenever

$$\begin{aligned} \omega &= 2M\pi/NT \qquad M \in \mathbb{Z} \\ f &= \frac{M}{N} f_r \end{aligned} \tag{14}$$

i.e. a notch appears at the revolution harmonic f_r whenever M is a multiple of N. Another observation is that the number of notches between 0 and f_r is N. Figure 6 shows the effectiveness of the notch filter. The revolution harmonic is suppressed by 50 dB.

A more important consideration is the phase around $\left(\ell + \frac{1}{2}\right) f_r, \ell \in \mathbb{Z}$ because our tunes are around here. The phase of the digital notch filter is

$$\arg\left[R_{\text{notch}}(\omega)\right] = \tan^{-1}\left(\frac{\sin \omega T}{1 - \cos \omega T}\right) \tag{15}$$

and for the case when $T = 2\pi/\omega_r$, $\arg\left[R_{\text{notch}}(\omega_r/2)\right] = 0$. Therefore, we can expand (15) about $\omega_r/2$ to get

$$\arg\left[R_{\text{notch}}(\omega)\right] = -\frac{\pi}{\omega_r}\left(\omega - \frac{\omega_r}{2}\right) + \mathrm{O}\left[\omega - \frac{\omega_r}{2}\right]^3 \tag{16}$$

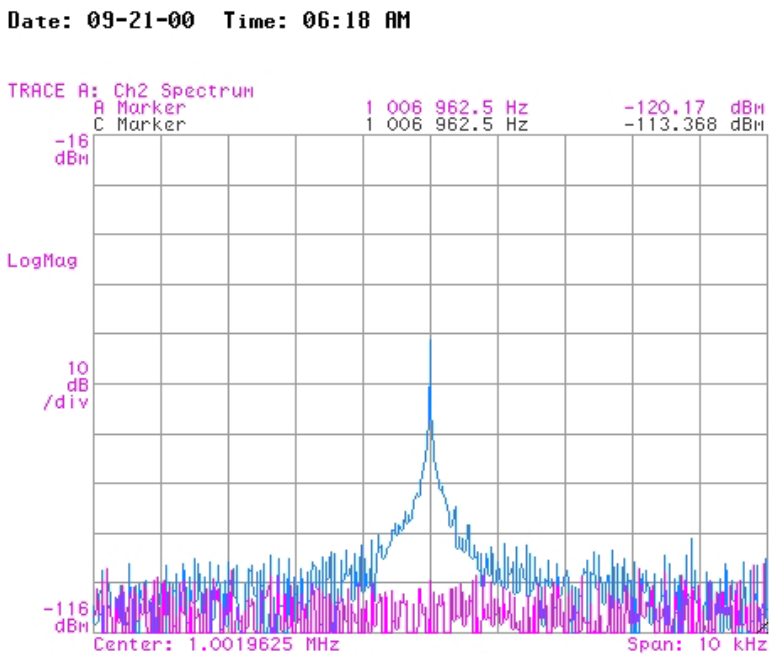

Figure 6 The notch filter suppresses the revolution harmonic by 50 dB.

Therefore, the small addition in phase for the horizontal tune sidebands for the Tevatron at 0.417 and 0.583 is $+15°$ and $-15°$ respectively. The same result applies for other values of ℓ.

Phase Advance

For damper operation, the phase advance ϕ_{pk} between the pickup and the kicker must be an odd multiple of $\pi/2$, i.e. $\phi_{pk} = \Delta\omega_q(T + t_{pk}) = (2n+1)\pi/2$ where $n \in \{0, 1, 2, \ldots\}$. If ϕ_{pk} is not an odd multiple of $\pi/2$, we can use two pickups to create a virtual pickup so that $\phi_{pk} = (2n+1)\pi/2$. Although, we are lucky to have a good enough phase advance for both the horizontal and vertical planes in our system, we will, nevertheless, go through the maths to see how we can make a virtual pickup with two pickups. A good enough phase advance here means that the shoulders around the real parts of the resonances of

Figure 7(b) do not go too negative and thus limit the amount of gain we have. In practice, $80^\circ < \phi_{pk} < 100^\circ$.

We can think of the beam as executing simple harmonic motion with betatron frequency $\Delta\omega_q$ and for our simple analysis we will ignore the beta functions at the pickup and kicker. Even in this simple analysis, we can write the voltage V_p seen at the pickup as a sum of δ-functions because the beam is only detected once per turn at the pickup, i.e.

$$\begin{aligned} V_p(t) &= \tilde{V_p} \sum_{n=-\infty}^{\infty} \cos(\Delta\omega_q t)\delta\Big(t - nT\Big) \\ &= \frac{\tilde{V_p}}{2}\left[\sum_{n=-\infty}^{\infty} e^{i\Delta\omega_q t}\delta\Big(t - nT\Big) + \sum_{n=-\infty}^{\infty} e^{-i\Delta\omega_q t}\delta\Big(t - nT\Big)\right] \\ \Rightarrow \qquad \mathcal{FT}\Big[V_p(t)\Big] = \tilde{V_p}(\omega) &= \frac{\tilde{V_p}}{2}\left[\sum_{n=-\infty}^{\infty} e^{i\Big(\Delta\omega_q - \omega\Big)nT} + \sum_{n=-\infty}^{\infty} e^{-i\Big(\Delta\omega_q + \omega\Big)nT}\right] \end{aligned} \tag{17}$$

where $T = 2\pi/\omega_r$ is the revolution period, We can apply the Poisson sum formula

$$\sum_{n=-\infty}^{\infty} e^{2\pi n\frac{\omega}{\omega_r}} = \omega_r \sum_{n=-\infty}^{\infty} \delta\Big(\omega - n\omega_r\Big) \tag{18}$$

to $\tilde{V_p}(\omega)$ and get

$$\tilde{V_p}(\omega) = \frac{\tilde{V_p}\omega_r}{2}\left[\sum_{\ell=-\infty}^{\infty} \delta\Big(\omega + \ell\omega_r - \delta\omega_q)\Big) + \sum_{\ell=-\infty}^{\infty} \delta\Big(\omega + \ell\omega_r + \delta\omega_q)\Big)\right] \tag{19}$$

where $\Delta\omega_q = N\omega_r + \delta\omega_q$, $N \in \mathbb{N}$. and we obtain a spectrum of betatron tune sidebands $\delta\omega_q$ around the revolution harmonics ω_r.

If the time separation between the pickup and kicker is t_{pk}, *but* we kick the beam 1 turn later, then the phase advance from the pickup to the kicker is $\phi_{pk} = -\Delta\omega_q(T + t_{pk})$ (the negative sign comes from the definition of the Fourier transform). Thus the voltage seen at the kicker is

$$\begin{aligned} V_k(t) &= \tilde{V_p} \sum_{n=-\infty}^{\infty} \cos(\Delta\omega_q t + \phi_{pk})\delta\Big(t - nT\Big) \\ &= \frac{\tilde{V_p}}{2}\left[e^{i\phi_{pk}} \sum_{n=-\infty}^{\infty} e^{i\Delta\omega_q t}\delta\Big(t - nT\Big) + e^{-i\phi_{pk}} \sum_{n=-\infty}^{\infty} e^{-i\Delta\omega_q t}\delta\Big(t - nT\Big)\right] \end{aligned} \tag{20}$$

Applying the same technique as before, we see that the Fourier transform of $V_k(t)$ is

$$\tilde{V}_k(\omega) = \frac{\tilde{V}_p \omega_r}{2} \left[e^{i\phi_{pk}} \sum_{\ell=-\infty}^{\infty} \delta\Big(\omega + \ell\omega_r - \delta\omega_q)\Big) + e^{-i\phi_{pk}} \sum_{\ell=-\infty}^{\infty} \delta\Big(\omega + \ell\omega_r + \delta\omega_q)\Big) \right] \quad (21)$$

The interpretation of these results show that when the phase advance from the pickup to kicker is ϕ_{pk}, then the upper sideband is rotated by $+\phi_{pk}$, and the lower sideband must rotate by $-\phi_{pk}$.

In particular if $\phi_{pk} = -\pi/2$, we can illustrate the response of a damped simple harmonic oscillator with sidebands at $\ell\omega_r$ and $(\ell+1)\omega_r$ when measured at the pickup. See Figure 7. Using what we have discussed above, the sidebands at $\ell\omega_r + \delta\omega_q$ and $(\ell+1)\omega_r + \delta\omega_q$ will rotate by $\phi^+_{pk} = -\pi/2$, and become real and positive at the kicker. Similarly, the sidebands at $\ell\omega_r - \Delta\omega_q$ and $(\ell+1)\omega_r - \Delta\omega_q$ must rotate by $\phi^-_{pk} = +\pi/2$ from the pickup to the kicker and they also become real and positive. To get damping, we have to multiply Figure 7(b) by -1.

Making a Virtual Pickup

Next, let us consider the case that we want to make a virtual pickup so that $\phi^+_{pk} = \pi/2$. In order to do this, we will use two pickups and vectorially add their responses so that a virtual pickup is created which has a $\pi/2$ phase advance between the kicker and it. Let the phase advance between the pickup and kicker be ϕ^+_1 for pickup 1, ϕ^+_2 for pickup 2, and ϕ^+_v for the virtual pickup. Then if we think of the frequency response as a vector in the Argand plane, we can write the beam response $\boldsymbol{R_1}$ and $\boldsymbol{R_2}$ at each pickup 1 and 2 as

$$\left.\begin{aligned} \boldsymbol{R_1} &= A_1 \begin{pmatrix} \cos\phi_1 \\ \sin\phi_1 \end{pmatrix} \\ \boldsymbol{R_2} &= A_2 \begin{pmatrix} \cos\phi_2 \\ \sin\phi_2 \end{pmatrix} \end{aligned}\right\} \quad (22)$$

where $A_1, A_2 \in \mathbb{R}$ are the magnitude of each of the responses. Define $\alpha_1, \alpha_2 \in \mathbb{R}$ to be the

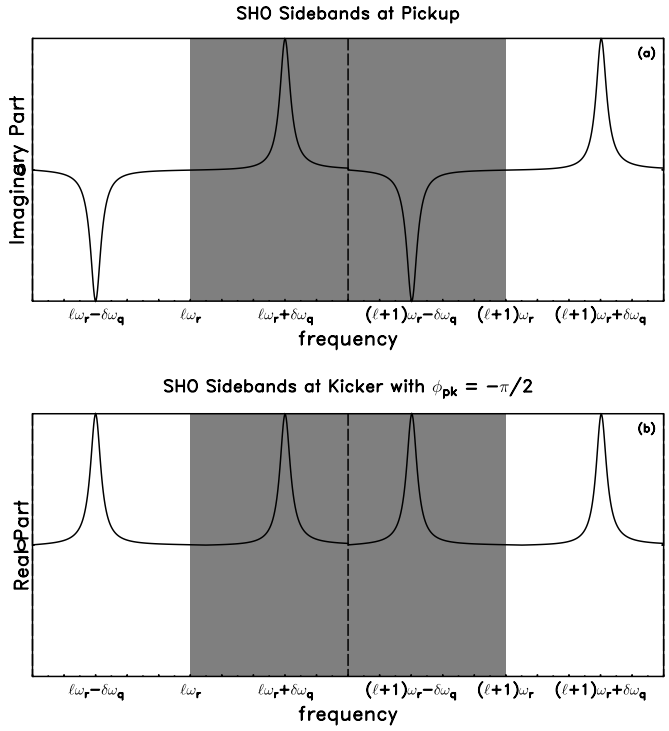

Figure 7 In graph (a), we show representative sidebands of a SHO about $\ell\omega_r$ and $(\ell+1)\omega_r$ when measured at the pickup. The shaded region shows the sidebands which we call the upper and lower tune sidebands about $\left(\ell+\frac{1}{2}\right)\omega_r$ i.e. the half integer. If $\phi_{pk}^{+} = -\pi/2$, then the sidebands from the pickup are rotated so that they are now real and positive at the kicker. See graph (b). The dashed vertical line is at $\left(\ell+\frac{1}{2}\right)\omega_r$.

parameters when determined produces the required virtual pickup, i.e.

$$\alpha_1 \boldsymbol{R_1} + \alpha_2 \boldsymbol{R_2} = \begin{pmatrix} \cos\phi_v \\ \sin\phi_v \end{pmatrix} = \begin{pmatrix} 0 \\ 1 \end{pmatrix} \qquad \text{if } \phi_v = \pi/2 \tag{23}$$

when solved for α_1 and α_2, gives us

$$\begin{pmatrix} \alpha_1 \\ \alpha_2 \end{pmatrix} = \frac{1}{\sin(\phi_1 - \phi_2)} \begin{pmatrix} \frac{1}{A_1}\cos\phi_2 \\ -\frac{1}{A_2}\cos\phi_1 \end{pmatrix} \tag{24}$$

Therefore, with the appropriate attenuation or amplifaction of the outputs of pickup 1 and

2, we have produced a virtual pickup with the desired phase advance between it and the kicker.

Delay through Electronics $T + t_{pk}$

The goal of of this section to show how we can set the delay in the damper system so that when we detect bunch n at the pickup, we will kick the same bunch n some time later. To ensure that we do indeed do this, we have to add cable to the damper electronics so that the the delay through the damper system is $T + t_{pk}$. See Figure 8.

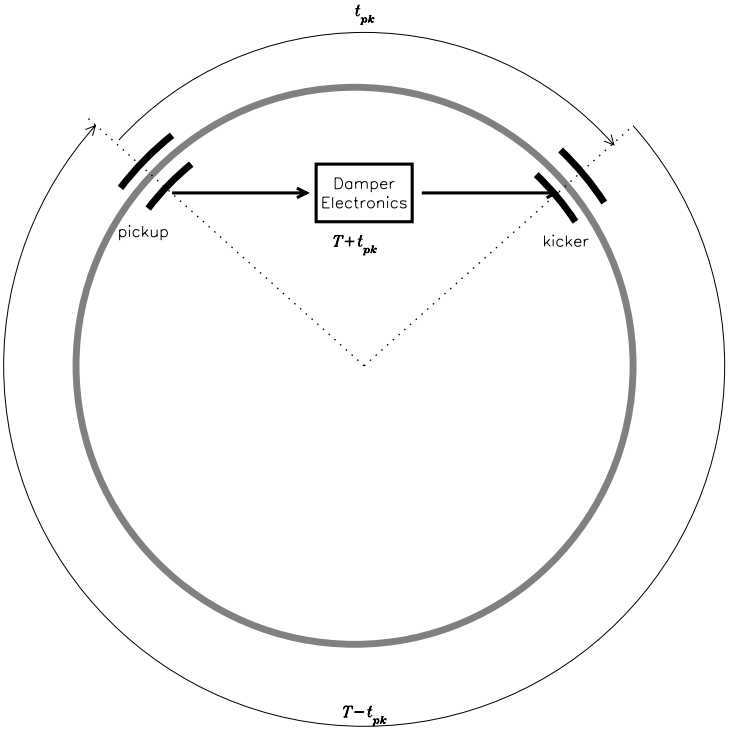

Figure 8 The transit time between the pickup and the kicker is t_{pk}. The delay through the damper electronics is $T + t_{pk}$, so that the bunch detected at the pickup is kicked one turn later.

In constrast with damper operation where we measure the beam position and then kick

the beam, when we do an open loop measurement, we kick the beam and then measure the position of the beam at the pickup. Thus, the phase is accumulated by going through the lower part of the ring of Figure 8 which has a time delay of $T - t_{pk}$, and then through the damper electronics which has a time delay of $T + t_{pk}$. Therefore the accumulated phase $\phi_{kp}(\ell)$ for every tune sideband is

$$\left.\begin{aligned} \phi_{kp}(\ell) &= -\Big[\Big(\ell\omega_r \pm \delta\omega_q\Big)\Big((T - t_{pk}) + (T + t_{pk})\Big)\Big]_{2\pi} \\ &= -\left[\pm 4\pi \frac{\delta\omega_q}{\omega_r}\right]_{2\pi} \end{aligned}\right\} \tag{25}$$

where $[.]_{2\pi}$ is the modulo 2π function. This means that when we get the delay *exactly* right, the upper sideband and the lower sideband have equal and opposite ϕ_{kp}.

Timing In Recipe

In practice, to time in the damper system which does *not* have $\phi_{pk} = (2n+1)\pi/2$, $n \in \mathbb{Z}$, we have to have two pickups A and B and do the following:

(i) Start with pickup A, by using the open loop response from pickup A to the kicker, adjust the electronic delay so that the real part of the upper sideband of every harmonic $\ell\omega_r$ looks the same. If the delay is right, the real part of the lower sideband of every harmonic $\ell\omega_r$ will also naturally look the same.

(ii) Calculate the phase advance ϕ_{pk} from the open loop response with the delay found using (i) by using the observation that the real part of the upper and lower sidebands look the same for every harmonic $\ell\omega_r$ if the phase advance between pickup and kicker is an odd multiple of $\pi/2$ it will look like Figure 7(b).

(iii) Repeat (i) and (ii) for pickup B.

(iv) Using the phase advances found for pickups A and B to the kicker, we can use equation (24) to create the virtual pickup which has an odd $\pi/2$ phase advance to

the kicker.

(v) Check that the open loop response with the virtual pickup to the kicker looks like Figure 7(b).

Uniform Triggers

In order for the digital delays to work they have to be triggered. The triggers which we use are uniform in time and they trigger in places even when the beam is not present. The reason will become apparent later in the discussion. At present, in Tevatron operation, there are three trains of 12 bunches each. In each train, the bunches are spaced 21 buckets apart. The spaces between the trains are the abort gaps and they take up 140 buckets each. The occupied buckets are as follows

$$\mathbf{1}, \mathbf{22}, \mathbf{43}, \ldots, \mathbf{211}, \mathbf{232} \quad | \quad \text{train 1}$$

$$\mathbf{372}, \mathbf{393}, \mathbf{414}, \ldots, \mathbf{582}, \mathbf{603} \quad | \quad \text{train 2}$$

$$\mathbf{743}, \mathbf{764}, \mathbf{785}, \ldots, \mathbf{582}, \mathbf{603} \quad | \quad \text{train 3}$$

Notice that all bucket spacings are divisible by 7. Therefore, if we have triggers which are spaced exactly 7 buckets apart, the digital delays will sample all the bunches as well as alot of empty space. The reason for having more triggers than necessary is to allow us to use reasonable cable delays to fine tune the system delay to ensure that the correct buckets are kicked. In the worst case scenario for this trigger pattern, the cable length will be 7 buckets/2 $\approx$ 70 ns for correctly hitting the right bucket. While for triggers where there are bunches only, the worst case scenario will be 140 buckets/2 $\approx$ 1.3 μs of cable! (Recall that 1 ns is about 1 foot of cable.)

RESULTS

We measured the open loop response of the damper system by breaking the loop as shown in Figure 9. The Tevatron is filled with 36 bunches of protons in the pattern discussed in *Uniform Triggers*. The frequency response as found at 150 GeV, is shown in Figure 10(a). After we add in 17 μs of delay, the frequency response becomes nice and symmetric about $f_r/2$ as shown in Figure 10(b). Compare this to Figure 7(b). In this case, it is quite obvious that the phase advance is close to $-90°$.

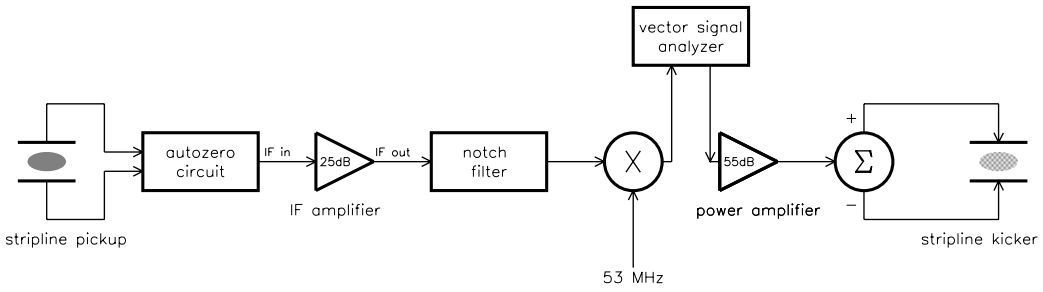

Figure 9 The loop is broken just downstream w.r.t. mixer and a vector signal analyzer (VSA) is connected there.

To calculate the phase advance between kicker to pickup, we have to make the imaginary part of the frequency response of Figure 10(b) look anti-symmetric about $f_r/2$ by taking out the phase advance. We find that the phase advance required to make the tune sidebands look antisymmetric is $-(85 \pm 5)°$. The result with $\phi^+_{pk} = -85°$ is shown in Figure 11. It is interesting to compare the experimental results with what was discussed under *Setup* and Figure 7.

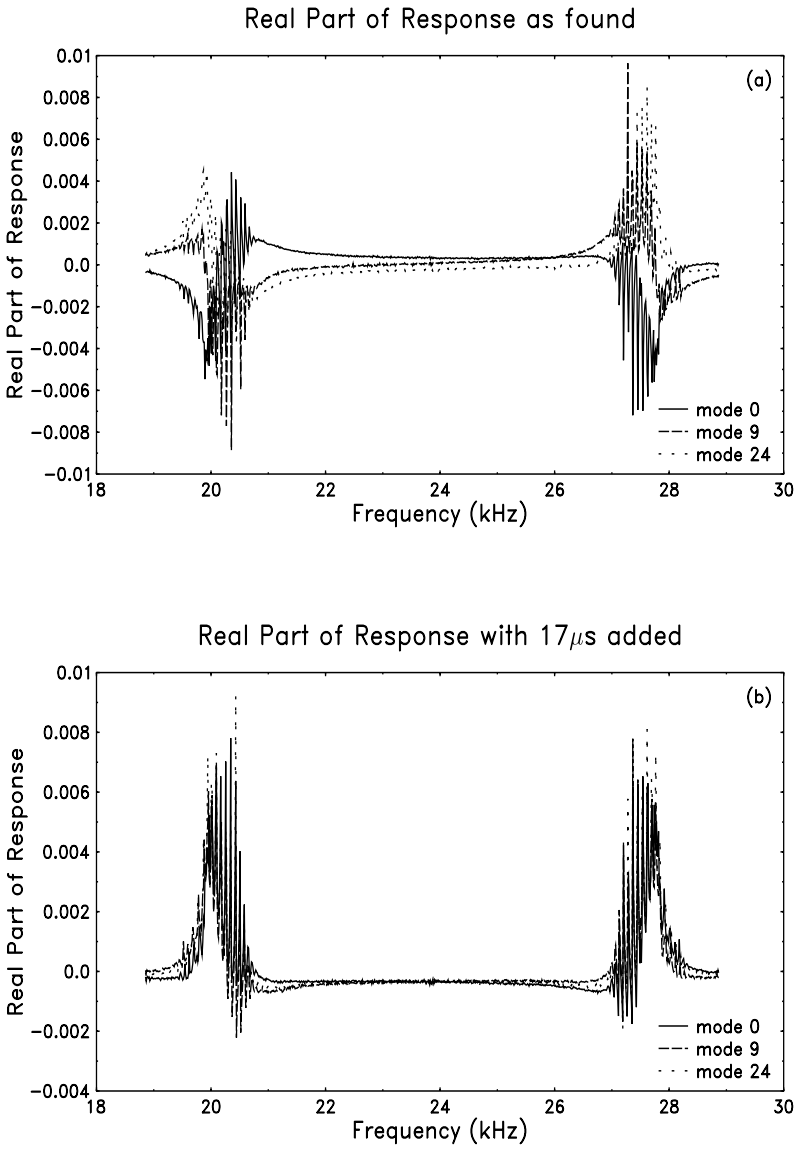

Figure 10 These graphs show real part of the response before and after adding 17 μs to the digital delay. To get the real part of the response to be negative, we have to multiply by -1 in the electronics. We have superimposed all the three graphs on top of each other by shifting the frequency of mode 9 by $-9f_r$ and mode 24 by $-24f_r$.

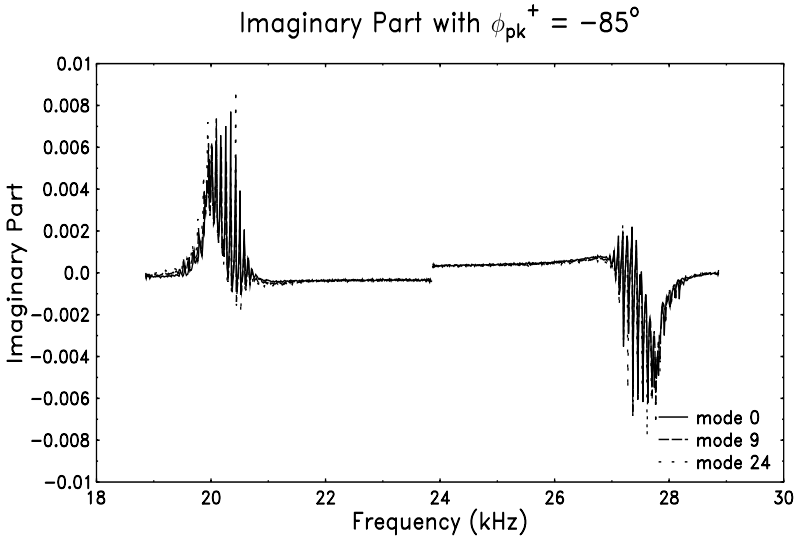

Figure 11 By taking out the phase advance of $-85°$, we can make the imaginary part of the response look anti-symmetric about $f_r/2$. Again, the three graphs have been superimposed each other by shifting the frequency of mode 9 by $-9f_r$ and mode 24 by $-24f_r$. The discontinuity at $f_r/2$ comes from a small DC offset in the original response data.

Comparing with *MAD* Input Data

We can compare our results to that of the *MAD* lattice file which has the theoretical ϕ^- values, i.e. the lower sideband w.r.t. f_r or the upper sideband w.r.t. $f_r/2$. The phase advance φ_{pk} from the pickup to the kicker as found in the lattice file *v3h01v2_new_new.lat* is $-43°$.† The total phase going one turn through the Tevatron is $\varphi_{\rm Tev} = -(20\times360+211)°$ and the phase from the notch filter for $\delta\omega_q/\omega_r = 0.583$ is $\varphi_f = -15°$. Adding these phases together, we obtain $\phi_{pk}^- = \Big[\varphi_{pk}+\varphi_{\rm Tev}+\varphi_f\Big]_{360°} = -\Big[269°\Big]_{360°} = +91°$. Thus $\phi_{pk}^+ = -91°$ which is extremely close to what we have measured $-(85\pm5)°$ from the previous section.

† If we had blindly used the lattice file and placed the pickup and kicker in the Tevatron so that the phase advance between them is $-90°$, then we definitely would have had to use two pickups because we had had forgotten to add the phase accumulated from one turn.

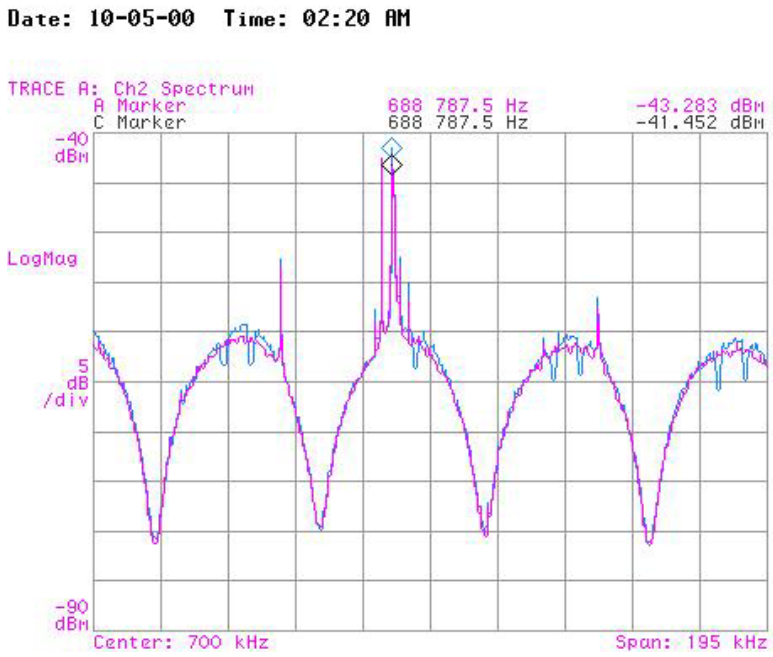

Figure 12 There is a huge noise spike at 688.8 kHz. This is cured by replacing RG58 cable with stripflex at the input and output of the IF amplifier (See Figure).

Dampers' Bane: Noise

So, the next obvious thing to do is to close the loop and watch the dampers do its thing. However, our first attempt turns out to be rather disappointing — noise plagued the system. The main sources of noise are:

(i) Digitization noise. It is well known that digitization produces quantization noise and it is the least significant bit which contributes to the noise floor. With the 14 bit ADC and DAC which we use, we expect the noise floor to be lower by -36 dB compared to an 8 bit system (at 6 dB per bit). In fact, it is extremely optimistic to assume that we can use all the bits. We discovered that the differential amplifier used just upstream of the ADC contributes about 3.5 bits of noise, which in effect, lowered the number of effective bits to 10.5 bits. In our defence, the

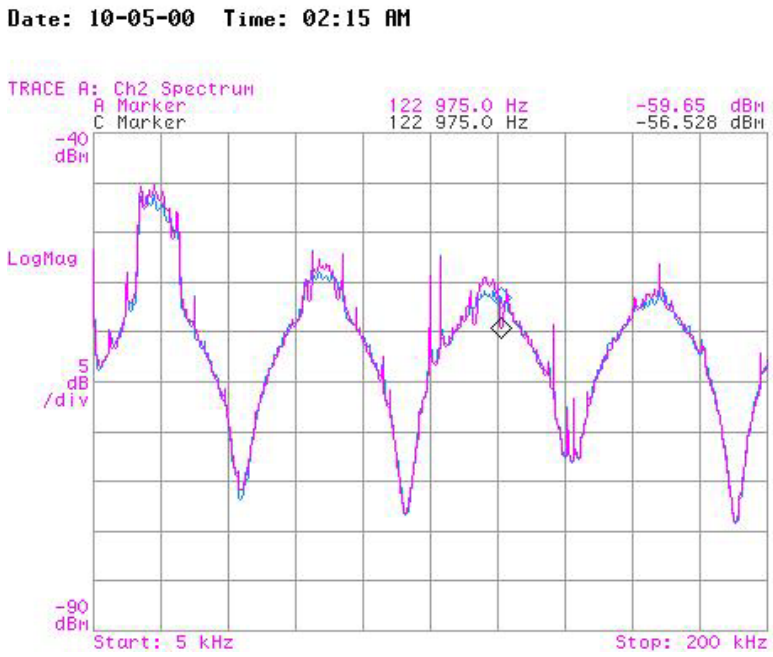

Figure 13 There is band of low frequency noise (between 10 to 15 dB) around 10 kHz. This comes from the pbar RF coupling into the proton RF.

choice of differential amplifier is recommended in the ADC reference design by Analog Devices.

(*ii*) Coupling between cables. RG58 is not good for systems with high gain because it does not have a very dense braid for shielding RF. Figure 12 shows a noise spike at 688.8 kHz which is cured by replacing RG58 cable with stripflex at the input and output of the IF amplifier (See Figure). Stripflex has two levels of shielding: a dense braid and a copper film winding which produces superior shielding. This results in a shielding efficiency of 90 dB compared to 40 dB for RG58.

(*iii*) General coupling from the "ether". The service building where the damper electronics are located has alot of background RF bouncing around. In particular, the low frequency band of noise shown in Figure 13 comes from the coupling of pbar RF located on a patchpanel into the proton RF on the same patch panel. The

solution is to relocate the pbar RF patchpanel into an adjacent rack.

With the damper noise under control, we found that the emittance growth from damper noise with the loop closed is $\sim 1\pi$ mm·mrad·hr^{-1} at 150 GeV.

Closing the Loop

Finally, we can close the loop and damp. We injected 36 bunches into the Tevatron and sat at 150 GeV for this set of experiments. Figure 14 shows the effect of closing the loop. The red curve is the noise spectrum measured at A of Figure 2 with the power amplifier off. The power amplifier is turned on, thus closing the loop, and we see that there is a suppression at the horizontal tune sidebands of about 6 dB (the purple curve). The noise floor is increased by about 2 dB in the middle of the spectrum. From the discussion in Appendix I, the closed loop gain of the damper is 6 dB at the horizontal tune. The full width at half min (fwhm) of the absorption line gives the damping time of the damper for the 361.6 kHz tune line which is 0.55 ms $\approx$ 26 turns in the Tevatron. (See Appendix I)

An immediate question which we wanted to answer is how sensitive is the damper to coherent motion of the beam. Clearly, we do not see the tune lines on the red curve of Figure 14 which means that the tune lines must be below the noise floor of the damper system which is -64 dBm. To see how sensitive our electronics are we injected RF at point A and measured at point B of Figure 15. The injected RF power is -100 dBm (purple curve) and the output power (blue curve) is > 10 dB above the noise floor.

To see what -100 dBm corresponds to in transverse position, we start with the usual relationship between transverse position Δx w.r.t. the electrical centre and the beam cur-

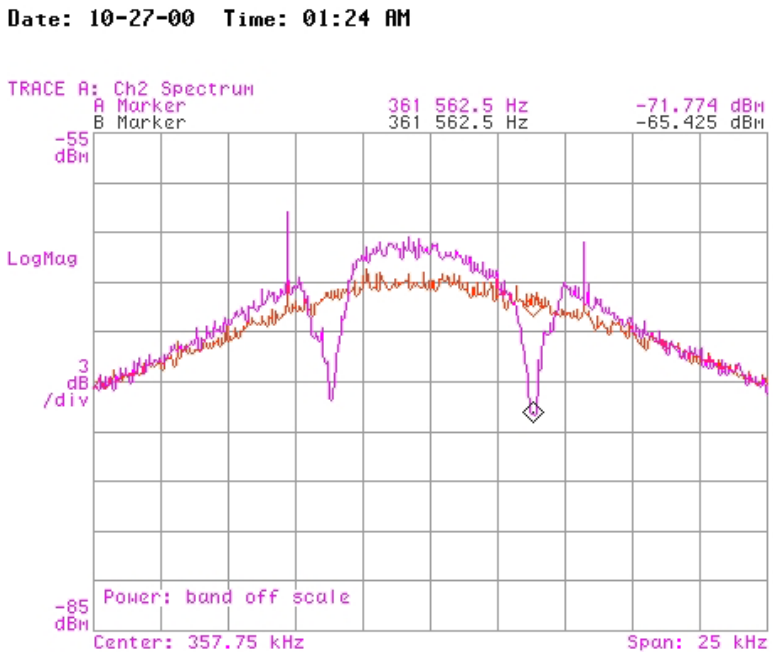

Figure 14 The suppression of the horizontal tune sidebands (purple curve) when the loop is closed compared to the red curve when it is open.

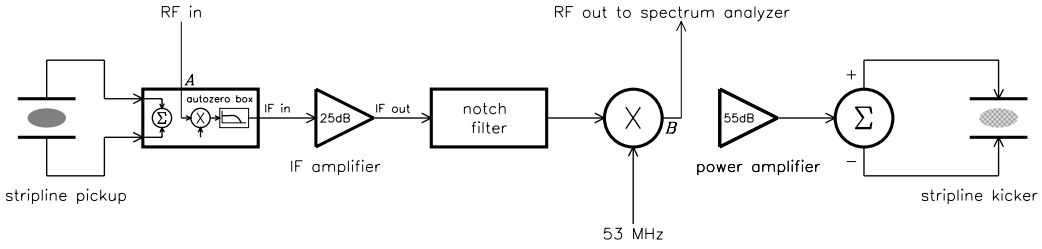

Figure 15 In order to measure the sensistivity of the electronics to coherent motion of the beam, we inject at A an RF signal which we then measure at B.

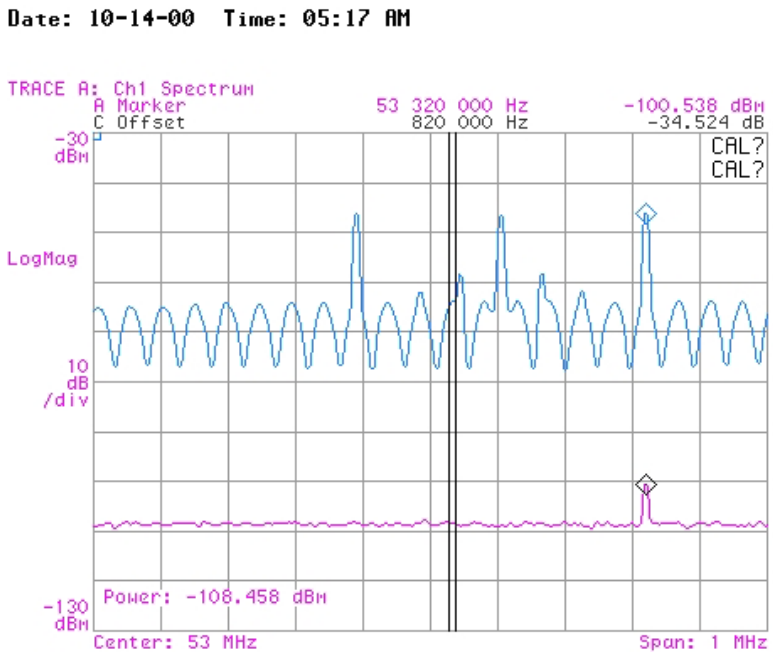

Figure 16 This shows the sensitivity of the dampers to coherent oscillations. The purple curve is the RF input at A and the blue curve is the output at B. The central peak of the blue curve is the leakage from the mixer of the proton RF.

rent I. The current on plate A and B are given by (See Figure 3)

$$\left.\begin{aligned} I_A &= \frac{I}{2}\left(1+\frac{2\Delta x}{d}\right) \\ I_B &= \frac{I}{2}\left(1-\frac{2\Delta x}{d}\right) \end{aligned}\right\} \tag{26}$$

where d is the distance between the two plates. The difference signal $\Delta I = (I_A - I_B) = 2I\Delta x/d$ and suppose the impedance the difference signal sees is Z, then the difference voltage induced by the beam is IZ and the rms power is thus $\Delta I^2 Z/2$ which in dBm is $10\log_{10}(\Delta I^2 Z/2\times 10^3)$. Putting in the numbers $Z = 50\Omega$, $I = 10$ A and $d = 3\times(2.54)$ cm, we obtain $\Delta x = 2\times 10^{-7}$ cm when the input power is -100 dBm. However, this is quite optimistic and we must take into account the attenuation of the cables (about 300 feet of heliax at 1dB/100ft between 30MHz to 200MHz) and attenuators (10 dB) of the autozero box. Doing so gives a more realistic value of 8×10^{-7} cm or 8 nm which is the size of the

coherent motion.

To prove that we are indeed damping the beam, we lower the horizontal chromaticity from its usual 8 units to -3.5 units with the horizontal dampers on and the beam remains stable throughout this exercise. However, when we turn the dampers off, the beam immediately goes coherent and falls out of the Tevatron.

Operations

In operations, we lower the horizontal chromaticity by about 6 units and vertical chromaticity by about 4 units from their nominals of 8 units for both planes on the central orbit and 12 units for the horizontal and 8 units for the vertical on the proton helix. For store #1868 shown in Figure 17 which had the horizontal chromaticity lowered by 5 units and vertical lowered by 2 units, the effect of the lower chromaticity is dramatic. Before the dampers are turned on, beam lifetime T:IBEAM (total beam current) and C:FBIPNG (proton beam current) is poor. The $1/e$ time is about 1 hr for C:FBIPNG at this time. When the dampers are turned on for pbar injection and chromaticities lowered, we see that the C:FBIPNG $1/e$ lifetime is improved by a factor of 3 to 3 hr. At the completion of pbar injection, just before we ramp, the dampers are turned off and chromaticities restored to nominal. Again, we see that the T:IBEAM and C:FBIPNG lifetime reverts back to being poor again.

It is interesting to note that for high energy operations, the choice of chromaticities is dictated by pbar lifetime. When we operate at low chromaticity, we lose about 1% of the pbars during injection compared to 10% with higher chromaticity. We cannot lower the chromaticities to too low a value because we do *not* have any transverse pbar dampers at this time. During injection the pbar chromaticity is around 2 and 4 for horizontal and vertical respectively because the nominal chromaticity on the pbar helix is about 8 for

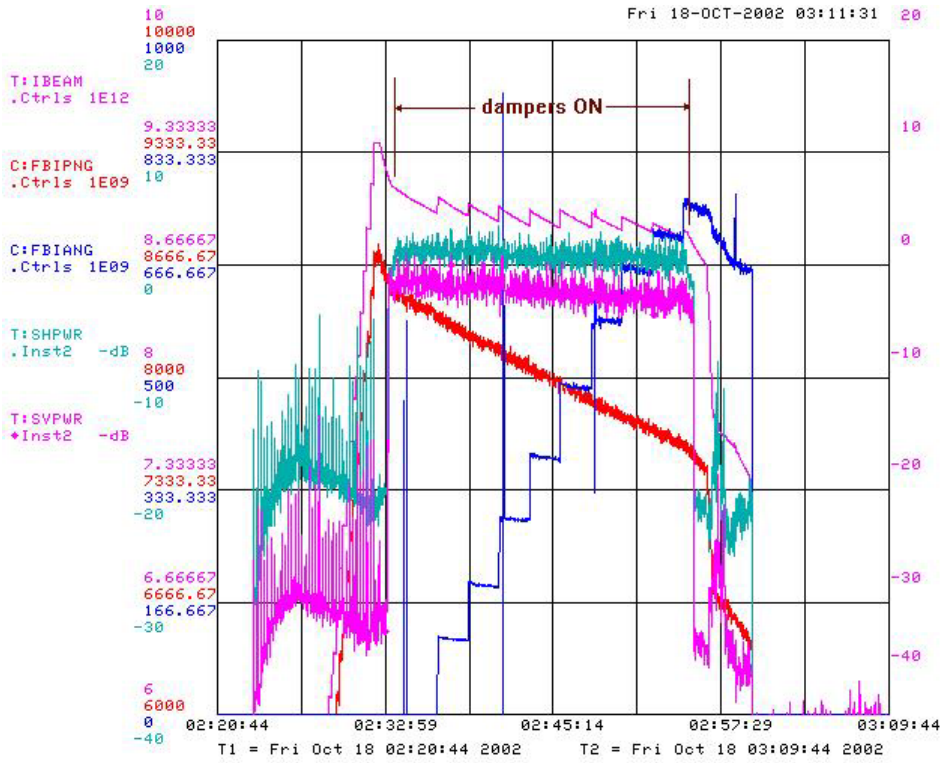

Figure 17 This plot shows the damper in action. Total beam current is T:IBEAM (the sawtooth shape comes from pbars being injected). C:FBIANG shows the increase in pbar current as they are being injected. C:FBIPNG is the proton beam current only. T:SHPWR and T:SVPWR are the horizontal and vertical Schottky powers which rise up by about 30 dB when the dampers are turned on.

both planes when the central orbit chromaticity is set to 8 for both planes.

Coupling

Coupling is an important issue when operating transverse dampers because we have two planes to worry about. We discover to our dismay (although we should not have been surprised) that if the Tevatron is not decoupled to a tune split to better than 0.005, the dampers of one plane will excite the other plane. Figure 18 clearly demonstrates the coupling problem.

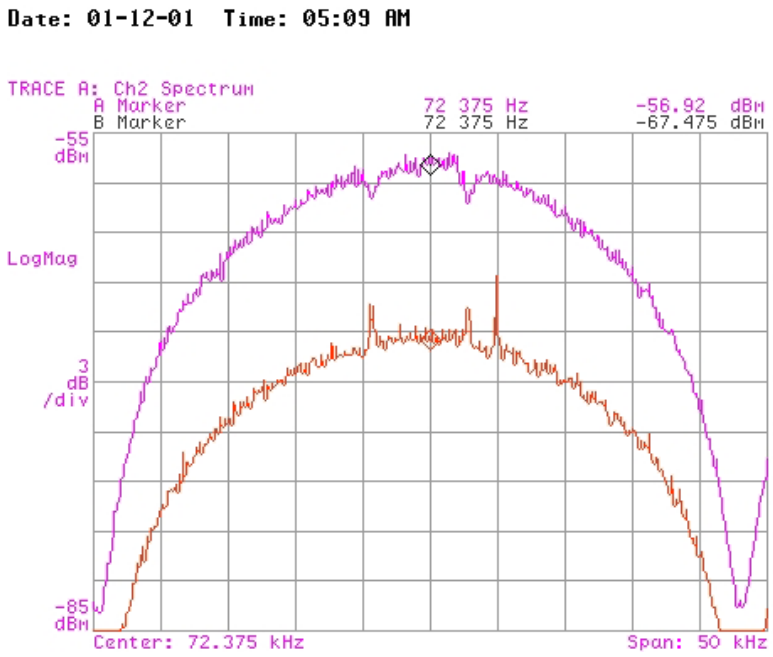

Figure 18 The purple curve shows damping in the vertical plane. However, the orange curve shows that the vertical damper is exciting the beam horizontally.

The purple curve shows that when the vertical damper is on and horizontal off, it produces tune suppression. However, the horizontal tune is excited. So, if we have dampers of both planes on, they tend to fight each other and cannot keep the beam stable when the chromaticity is lowered.

Mysteries

We catalogue here some observations which, at present, we have no answers for.

(i) The dampers described in this paper can only damp rigid coupled bunch modes. It does not have the bandwidth to damp head-tail modes. This is easily demonstrated by lowering the horizontal chromaticity of a single bunch until it becomes unstable and falls out. With or without the dampers, for a single bunch, when the horizontal

chromaticity is about 2 units, the bunch becomes unstable and falls out. This is consistent with our dampers not being able to keep head-tail modes stable. However, when we have 36 bunches in the Tevatron, the beam remains stable even when we lower the chromaticity to negative values. This seems to indicate that the single bunch instability threshold has been modified when there are 36 bunches in the Tevatron.

(*ii*) Lowering the chromaticity does not always improve the lifetime of the proton beam despite Figure 17. The naïve idea that by lowering the chromaticity, the footprint of the beam in the tune plane becomes smaller and thus enclosing fewer resonances, and therefore improving the lifetime does not seem to be borne out every time. Some unknown essence of the proton beam seems to be just as important as the value of the chromaticity. However, as was discussed earlier in *Operations*, at times the dampers do improve the lifetime. Note that unlike the proton beam, the pbar beam lifetime is always improved with lower chromaticity. *Update 19 Dec 2002 to 12 Jan 2003 (shutdown): The proton beam lifetime is improved dramatically* ($\times 5$) *on the proton helix all the time when the chromaticity is lowered. Somehow the proton behaviour has changed after our feeddown decoupling work on the helix compared to stores before this date.*

CONCLUSION

The transverse dampers have been used in high energy physics operations and enough data have been gathered to show that the dampers do no harm to the protons or pbars at 150 GeV. With low chromaticity the lifetime of the pbars is always improved, although the proton lifetime is improved some of the time on the helix. Thus the value of the dampers for high energy operations is mainly for keeping pbars in the Tevatron during injection. However, mysteries remain, which when solved will enable us to assess the operation of the transverse dampers better.

APPENDIX I

In this appendix, we will derive the $1/e$ time and the gain of the damper from its frequency response. Suppose the open loop response of the damper is described by a constant gain G and a damped simple harmonic oscillator (SHO). See Figure 19. In the time domain, the equation of motion of a damped SHO is

$$\ddot{x} + \lambda\dot{x} + \omega_0^2 x = F(t) \tag{27}$$

where λ is the damping constant which comes from the damper, ω_0 the natural frequency of the SHO and $F(t)$ some external forcing function. Without loss of generality, let us suppose that at $t = 0$, $x(0) = \dot{x}(0) = 0$, then the Laplace transform of (27) trivially yields the response function

$$H_{\text{sho}} = \frac{1}{s^2 + \lambda s + \omega_0^2} \tag{28}$$

This, then gives us the open loop response H_{open}

$$H_{\text{open}} = GH_{\text{sho}} = \frac{G}{s^2 + \lambda s + \omega_0^2} \tag{29}$$

When we close the loop, we see that the closed loop response H_{closed} is

$$H_{\text{closed}}(s) = \frac{1}{GH_{\text{sho}}(s)} = \frac{1}{G}\left(s^2 + \lambda s + \omega_0^2\right) \qquad \text{if } G \gg 1 \tag{30}$$

which basically tells us that the closed loop response produces an absorption spectrum when measured on a spectrum analyzer. In other words, the resonant spectrum of (29) becomes an absorption spectrum in (30) when the loop is closed.

So by using our knowledge of the resonant spectrum, we can deduce the usual parameters that describe the damper when we use the absorption spectrum instead. The $1/e$ damping time is given by $\lambda = 2Q/\omega_0$ where $Q = \omega_0/\Delta\omega_{\text{fwhm}}$, $\Delta\omega_{\text{fwhm}}$ is the full width of the frequency at half the *minimum* amplitude. And finally, the maximum gain of the loop is the inverse of the minimum amplitude.

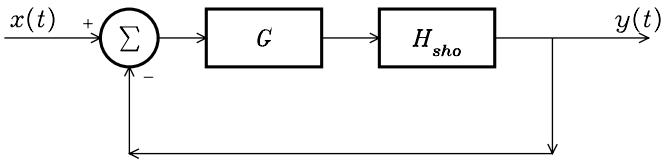

Figure 19 This is a block diagram of a damper for a simple harmonic oscillator where the open loop response is $GH_{\rm sho}$.

REFERENCES

[1] *2002 Tevatron Log Book*, Y. Alexahin, B. Hanna, J. Annala, C.Y. Tan, 2002.

[2] *Physics of Intensity Dependent Beam Instabilities*, K.Y. Ng, FN-0713.

[3] *Introduction to RF Systems*, D. McGinnis, 1995 U.S. Particle Accelerator School, Duke University, 1995.